Journal of Earth Sciences and Geotechnical Engineering, vol. 5, no.4, 2015, 57-77
ISSN: 1792-9040 (print), 1792-9660 (online)
Scienpress Ltd, 2015

An Engineering Site Characterization using Geophysical Methods: A Case Study from Akure, Southwestern Nigeria

Yusuf Gbenga Ayodele[1], Akinrinade Opeyemi Joshua[2], Ojo John Sunday[3]

Abstract

An engineering site characterization using geophysical methods namely Very Low Frequency (VLF) electromagnetic, Vertical Electrical Sounding (VES), and magnetic methods have been completed at a site located at Aba-Oyo area, Akure. This was aimed at evaluating the geoelectrical, magnetic and electromagnetic parameters of near surface earth materials and its engineering implications, towards the construction of an engineering structure. Ten VLF and magnetics profiles were occupied, with traverse length varying from 50-70 m; and twelve VES positions across the study area. Quantitative interpretation was initially carried out on the VES using the partial curve matching technique and 1-D forward modelling with Win Resist software. Quantitative interpretation of the VLF revealed some conductive zones which were characterized as geologic structures such as fractures, faults, and lineament which can serve as pathway for fluid flow. Four lithologic units were delineated namely top soil, lateritic layer, weathered layer and fresh basement. The top soil resistivity varies from 44-181 Ωm and thickness ranges between 0.4 and 2.0 m, lateritic layer resistivity varies between 20-174 Ωm and thickness ranges between 1.7-5.2 m, while the weathered layer resistivity varies between 20-310 Ωm and thickness between 1.4-7.4 m. Bedrock ridges and depressions were identified on the overburden thickness map. Low resistivity values of the top soil suggest high clay content. Result shows that the subsurface earth materials differ in their competency due to the variation in resistivity value. Possible source of failure identified include incompetent earth layers characterized by low resistivity, laterally inhomogeneous subsurface layer and conductive zones identified as fractures and faults. It is concluded that a high rise building or structure with a strip footing foundation will require engineering intervention such as pilling to a depth of about 8-12 m.

Keywords: Foundation studies, Electrical Resistivity, VLF, engineering geophysics

[1]Department of Applied Geophysics, Federal University of Technology Akure, Nigeria
[2]Department of Marine Science and Technology, Federal University of Technology Akure, Nigeria
[3]Department of Applied Geophysics, Federal University of Technology Akure, Nigeria

1 Introduction

Detail understanding of the geoelectric properties of the subsurface earth material and its engineering implications is important in pre-construction foundation studies. The result of such study should be utilized at the project planning phase to prevent potential structural failure and loss of valuable asset. Geophysical methods have been found very relevant in construction of engineering structures due to its non-intrusive approach to civil engineering site investigation, relatively low cost and time saving advantage.

In many parts of the world, lives have been lost and casualties recorded as a result of structural failure. Common structural failures in the world today include failure of bridges, dams and buildings, which is the most prominent of all. Records of such structural disasters are common in Western Canada, Colorado, Texas, Wyoming, India, Nigeria, Israel, South Africa, and to some extent South Australia, California, Utah, Nebraska and South Dakota most of which were associated with expansive soils [1][2].

Structural failure is said to have occurred when there are unacceptable differences between expected and observed performance of any structure. The cause could be from a natural cause relating to tectonic activities which takes place in the earth e.g. earthquake, tremor, faulting and folding; while it could also be as a result of clay content of the top soil, heterogeneous nature of the sub-base and sub-grade materials, poor quality of building materials, old age of building, and failure precipitated by differential settlement, differences in expansion and compression coefficients of construction materials, relative changes in the shapes and sizes of saturated soils [3][4][5][6][7][8] and errors in structural design. The incompetent earth layers could be related to differential settlement, fractures, faults, joints and lineaments structures underlying the construction site. Understanding the subsurface geology prior to construction will therefore provide the required information to prevent structural failure.

When the foundation of an engineering structure is erected on less competent earth layer, it poses serious threat to the structure and can also lead to its collapse. Thus, need to evaluate the subsoil integrity prior to construction. The durability and safety of engineering structural setting depend on the characteristic of the subsurface earth materials and the mechanical properties of the overburden.

Pre-construction foundation studies will reveal potential future subsurface problems and assist in providing possible solutions before erecting a building [9]. Such result will serve as baseline information which is invaluable. The aim of this research is to evaluate the depth and spacial extent of the geoelectric, magnetic and electromagnetic parameters in the study site, and identify subsurface features which may be inimical to foundation integrity.

2 Description of the Study Site

The study site is located around Aba-Oyo area FUTA south gate, Akure (Figure 1). It is accessible through FUTA road via the Stateline Hotel junction. The area is bounded by Longitude 5^0 9’ 13.09” E, and 5^0 9’ 11.72” E, and Latitude 7^0 17’ 12.83” N and 7^0 17’ 13.42” N. It is geographically located within the sub-equatorial climate belt of tropical rain-forest vegetation with evergreen and broad-leaved trees. It is characterized by uniformly high temperature, heavy and well distributed rainfall throughout the year. The

mean annual temperature is 24 - 27 ^{0}C, while the rainfall, mostly conventional, peaks twice in July and September and varies between 1,500 mm and 3,500 mm per year.

2.1 Geology of the Study Area

The study area is underlain by crystalline rocks of Precambrian Basement Complex of Southwestern Nigeria [10][11][12]. The crystalline rocks are porphyritic granite, biotite granite, quartzite and qneiss migmatite. Gneiss migmatite and biotite granite are the major outcrop, while Charnockite rocks occur as discrete bodies within the study area. The geology and boundaries of the lithological units were inferred in places where they are concealed by superficial residual soil (Figure 2).
The fractured bedrock generally occur in a typical basement terrain [13] in tropical and equatorial regions while weathering processes create superficial layers, with varying degree of porosity and permeability. Research findings shows that unconsolidated overburden could constitute reliable aquifer if significantly thick [14][15[16]. Thus, the lithological units present include Migmatic gneiss complex, granitic gneiss and Charnokites. Outcrops of biotite gneiss and granitic gneiss occur in some locations around the western part of the study area. Likewise some boulders of granite and charnokites were observed at the western part of the study area.

3 Methodology

The following equipment were used in the acquisition of field data for this project work: Ohmega resistivity meter, Reels of cables, Compass-clinometer, Hammers, Measuring tape, galvanized electrodes, Garmin Global Positioning System (GPS), Proton precision magnetometer, and ABEM WADI VLF electromagnetic; while Karous Hjelt filter, Win-Resist and surfer were used in data processing, modeling and visualization. The investigation was initiated by preparing the location map, after which traverses were cut. A total of ten traverses were prepared with five in North-South (NS) and other five East-West (EW) orientation respectively. 10 m and 15 m inter traverse spacing was used for the NS and EW traverses respectively (Figure 3).

3.1 Theory of Electrical Resistivity Method

In the electrical resistivity survey, artificially generated electrical currents are passed into the ground and the resulting potential differences are measured at the surface. The technique explores the fact that there is a large contrast in resistivity of ore bodies and their surrounding host rocks. Two electrodes are used to supply a controlled electrical current to the ground. The lines of current flow adapt to the subsurface resistivity pattern so that the potential differences between the two points on the ground surface can be measured using a second pair of electrodes. Deviations from the pattern of potential differences expected from a homogenous ground provide information on the form and electrical properties of subsurface inhomogeneities.
The instruments introduces controlled current into the ground through metal electrodes and measures the resultant potential difference between the potential electrodes, and displays the internally computed resistance value and/or the current (in Amperes) and

potential (in Volts). Thus, the output resistances are average values over a number of cycles from each of these resistances; the apparent resistance for a particular spread length is computed using the relevant geometric factor (K). For combined strength and resistance to corrosion, galvanized steel electrodes are normally used. Four electrodes and four cable reels are required for conventional survey. Vertical Electrical Sounding Technique (VES) technique was adopted. A total of Twelve (12) stations were occupied. The current electrode (AB/2) was varied from 1-65 m. Schlumberger electrode configuration field operational procedure used involves expanding the current and potential electrodes about a fixed centre.

$$\rho_a = K\left(\frac{V}{I}\right) \tag{1}$$

Where $\rho_a$is the apparent resistivity, K, V and I are the geometric factor, voltage and current respectively.

3.2 Very Low Frequency Electromagnetic Method

VLF EM method detects electrical conductors by utilizing radio signals in the 15 to 25 kilohertz (kHz) range that are used for military communications. It is useful for detecting long, straight electrical conductors, such as moderate to steeply dipping water-filled fractures or faults. The VLF instrument compares the magnetic field of the primary (transmitted) signal to that of the secondary signal (induced current flow within the subsurface electrical conductor). In the absence of subsurface conductors the transmitted signal is horizontal and linearly polarized. When a conductor is crossed, the magnetic field becomes elliptically polarized and the major axis of the ellipse tilts with respect to the horizontal axis [17]. The anomaly associated with a conductor exhibits a crossover. As with other frequency domain electromagnetic systems, both the in-phase ("real" or "tilt-angle") and the out-of-phase ("imaginary," "ellipticity," or "quadrature") components are measured.

Data were collected along the traverses, and recorded anomalies were correlated from traverse to traverse. In planning the VLF survey several considerations were taken into account. Traverses were oriented in the dip direction so that the anomalous zones can be isolated and compared with background levels; while the traverses along the strike provide the lateral extent of the anomaly. Efforts were made to avoid potential sources of cultural noise which could mask anomalies associated with the intended target. Furthermore, consideration was given to available transmission station available for use during the survey. The direction toward the transmitting station was ensured to be nearly perpendicular to the traverse, while the grid is design to ensure correlation of anomaly across lines. The traverses covered the entire site, and the readings were ensured returned to a background level before another station data was acquired. Precautions required to ensure error associated with data acquisition is minimized was carefully observed.

Data filtering was carried out to enhance the signal and make tilt-angle crossovers easier to identify. Two commonly used filtering methods include the Fraser filter [18] and the Karous-Hjelt filter [19]. The Fraser filter simply converts tilt-angle crossovers into peaks. The Karous-Hjelt filter calculates the equivalent source current at a given depth, commonly known as current density. The current density position aids in the interpretation of the width and dip of a fracture with depth. Commercial programs are

available to calculate and plot data using the Karous-jelt filter. Current density was plotted with respect to depth with the aid of Karous-Hjelt program to create a pseudo-section for further interpretation.
By stacking sets of profiles it is then possible to correlate and identify fractures or conductive zones across the entire study site. Once the strike direction of a fracture has been determined, the fracture can be projected along strike to determine if it intersects any areas of interest. Qualitative interpretation was carried out on the processed VLF data, after plotting the "real" and the "imaginary" components against station distances along the traverses.

3.3 Magnetic Method

Magnetic prospecting method measures the sub-surface spatial distribution of rock magnetisation properties, J, which is also known as susceptibility or remanence which causes small changes in the earth's magnetic (Geomagnetic) field strength and direction. The objectives of magnetic data reduction include removing the long wavelength regional field so as to isolate the short wavelength residual field which is due to magnetic material that may be present on the site prior to determination of derivatives. This processing step was applied to the data obtained in the respective profiles. Also, horizontal derivative was derived to enhance the anomaly such that the edge can be accurately resolved. In this processing, the anomaly was assumed to be dispersed in the field and not necessarily in a particular orientation we are familiar with. Furthermore, the data was also not reduced prior to computing the derivatives.
The traverses 1 to 10 were individually processed and quality controlled. The result of the processed data was plotted on the field base map to produce 2D magnetic anomaly maps.
Horizontal Gradient (XDR): The horizontal gradient is denoted as**:**

$$\text{XDR} = \frac{\partial T}{\partial x} \tag{2}$$

Where T is the total field and x is distance along the profile line. The result is plotted against station locations while the maximum and minimum inflection in the 2D map is used in delineating the edges of magnetic materials on the field. Moreover, since the XDR is affected by dipping magnetic bodies it has limited application until it has been reduced to the pole. Therefore, it is not a strong indicator of location and has low sensitivity to noise. The horizontal gradient uses only horizontal derivatives and is therefore insensitive to noise and aliasing [20].

4 Results and Discussions

The results obtained from this study are presented as profiles, pseudo-sections, depth sounding curves, geo-electric sections, 2D resistivity maps, iso-resistivity depth slice, overburden thickness and table.
The raw real and the filtered real component of the VLF data─were interpreted qualitatively and semi-quantitatively (Figure 4a-4c). The varying amplitude of the VLF profile represents changes in the conductivity of subsurface earth materials, while the pseudo-section represents the conductivity changes along the profiles with respect to

depth. The peak positive amplitude of the filtered real indicate the presence of conductive bodies. Thus, the disposition of the conductive anomalies identified on the pseudo-sections is attributed to factures, faults and lineaments structures.

Three major resistivity sounding curves types were obtained namely H, KH, and HA type curve (Table 1, Figure 5). Results obtained delineate three to four lithologic units namely: topsoil, lateritic layer, weathered layer, and fresh basement. The results obtained from the quantitative interpretation of the sounding curves were used to generate the geo-electric sections (Figure 6). The geo-electric sections represent the geologic sequence mapped with respect to depth. It shows the lateral continuity of each delineated sequences across the VES stations.

Geoelectric profiles along traverse three, five and an arbitrary line are presented here. Profile along traverse 3 is in the S-N orientation and passes through VES 7, 8, 9 and 10. It represent four geologic sequence in which layer two shows a depression towards the north and south as a result of the rise in the weather layer at VES 8. A bedrock depression is observed around VES 9 at a depth of BOUT 10.9 m (Figure 6a). Profile along traverse five is in the S-N orientation, and involve VES 4, 5 and 6. The geoelectric section along traverse five reveals a laterally continuous top soil, which thins out towards VES 4 at the southern part. The lateritic layer identified at VES 4 thins out towards VES 5. The bedrock is observed to dip towards the southern part (Figure 6b). Arbitrary line extending from VES 4 to VES 3 shows a laterally continuous top soil. The bedrock expression shows a rise around VES 12 and VES 11, forming depression at VES 4, 8 and 3 (Figure 6c). Generally the resistivity value of the weathered layer is low.

Iso-resistivity depth slice was generated at 0.5m, 2m, 4m and 6m respectively. At 0.5 m, the earth materials reveal a generally low resistivity values which ranges between 40 Ωm and 180 Ωm (Figure 7a). The resistivity values in the north-west and south is low, and straddled between it is a high resistivity section oriented in the NE-SW direction. The resistivity values of the earth materials contained within the top soil can be classified as sand, clayey sand, sandy clay, and clayey formation.

At 2 m depth, the resistivity distribution is generally high on the southern flank with values which range from 120 Ωm to 190 Ωm (Figure 7b). This can be attributed to slightly competent earth materials, as compared with the northern flank with low resistivity values which range between 20 Ωm and 70 Ωm. The material type associated with the low resistivity values are clayey and sandy clay materials. This differential compaction of the materials could influence structural failure; therefore reinforcement of the foundation might be required at this depth. At 4 m, the resistivity value is ranges between 20 Ωm and 100 Ωm (Figure 8a). However, a high resistivity closed contour is observed on the eastern flank, which peak around VES 11. At 6 m depth, the resistivity distribution is generally less than 200 Ωm (Figure 8b), except on the west and eastern flank which exhibit high resistivity value, representing top of the basement rock.

The thickness map of the top soil varies between 0.4 m and 2.0 m. The north-west shows the highest thickness, and the south-east have an average thickness which range between 0.9 m and 1.1 m. In between the south-east and the north-west is straddled a low thickness zone, with orientation along the NE-SW and thickness range between 0.4 m and 0.9 m (Figure 9A).

The study site overburden thickness ranges between 4.3 m and 11.1 m. This was computed from the layer thicknesses of the VES across the study area (Figure 9b). The study site reveal a relatively thick overburden, except at the eastern part which exhibit the lowest recorded thickness (around VES 11).

The residual magnetic anomaly map (Figure 10b) depicts the magnetic susceptibility which characterizes the mineral constituents of the earth materials at the site, since no buried magnetic object is observed at the site. Low residual magnetic values were on the south and the north-east. However, a high susceptibility structure which extends from the east to the west and the north-west was also identified. This magnetic property represents the mineral constituents of the earth material in the site. The horizontal derivative (Figure 10b) reveal a localized low magnetic susceptibility at the west and south-west of the field, while a localized high is observed at the south-east. This anomaly on the west can be related to the shallow depth of the bedrock as presented in the overburden thickness map (Figure 9b). However, the map shows a generally flat horizontal derivative.

There is a direct relationship between electrical resistivity of earth materials and the subsurface capacity to sustain an engineering structure. Areas with low electrical resistivity representing clay, sandy clay and clayey sand materials are considered non competent. Areas associated with high conductivity as reflected in the peak positive amplitude of the VLF profiles and the pseudo-sections are considered to be zones of weaknesses such as fractures, faults, and lineaments; and are unfavorable to siting engineering structures. The bedrock topography reflects some undulating disposition which must be carefully considered in the foundation design to ensure stability of the structure.

5 Conclusion

The electrical resistivity method has been found very useful in delineating subsurface geologic features. Obtained results established the existence of four geologic layers consisting of top soil, lateritic layer, weathered layer and the fresh basement. Integrating VLF EM further improved the quality of the study and the precision with which subsurface structures such as fractures, faults and lineaments can be mapped. It is effective in mapping conductive formations or conductive zones which are inimical to engineering structures. The pseudo-section revealed both the lateral and the depth extent of the subsurface structures.

Information gathered from the neighborhood of the study site report the case of a collapsed structure adjacent to the site. The cause of the collapse might be due to siting the foundation on differential settlement. Construction of a high rise building or foundation with continuous footing therefore requires an engineering intervention such as pilling to a depth of about 8 – 12 m.

References

[1] Blyth, F.G.H. and de Freitas, M.D., “A Geology for Engineers,” Butler and Tannar, Ltd. Frome and London: London, UK, 1988.

[2] Mokhtari, M., and Dehghani, M., “Swell-Shrink Behavior of Expansive Soils, Damage and Control,” Electronic Journal of Geotechnical Engineering, Bund R. **Vol. 17**, (2012), 2673-2682.

[3] Oladapo M.I., "Geophysical investigation of road failures in the Basement Complex area of Ondo State Unpublished M.Tech. Thesis", Department of Applied Geophysics, Federal University of Technology, Akure, 1997.
[4] Ofomola, M.O., Adiat, K.A.N., Olayanju, G.M. and Ako B.D., "Integrated Geophysical Methods for Post Foundation Studies, Obanla Staff Quarters of the Federal University of Technology, Akure, Nigeria," Pacific Journal of Science and Technology, **Vol. 10**(2), (2010), 93-111.
[5] Oyedele K.F. and Olorode D.O., "Site Investigations of Subsurface Conditions Using Electrical Resistivity Method and Cone Penetration Test at Medina Estate, Gbagada, Lagos, Nigeria," World Applied Sciences Journal, **Vol. 11**(9), (2011), 1097-1104
[6] Lateef T.A. and Adegoke J.A., "Geophysical Investigation of Foundation Condition of a Site in Ikere-Ekiti, Ekiti State, South-Western Nigeria," Australian Journal of Basic and Applied Sciences, **Vol. 5**(9), (2011), 1852-1857.
[7] Egwuonwu G.N., and Sule. O., "Geophysical Investigation of foundation failure of a leaning superstructure in Zaria Area, Northern Nigeria," Research Journal in Engineering and Applied Sciences, **Vol. 1**(2), 2012, 110-116.
[8] Adelusi A.O., Akinlalu A. A. and Nwachukwu A. I, "Integrated geophysical investigation for post construction studies of buildings around School of Science area, Federal University of Technology, Akure, Southwestern, Nigeria," International Journal of Physical Sciences, **Vol. 8**(15), (2013), 657-669.
[9] Ibitoye F.P., Ipinmoroti, F.V., Salami M., Akinluwade K.,J., Taiwo, A.T., Adetunji, A.R., "Application of Geophysical Methods to Building Foundation Studies," International Journal of Geosciences, **Vol. 4**, (2013), 1256-1266.
[10] Rahaman M.A., "A Review of the Basement Geology of Southwestern Nigeria In Kogbe, C.A. (Editor)," Geology of Nigeria, Elizabethan Publishing Co., 1976.
[11] Adegoke O.S., "Thethyan affinities of West African Paleogene Molluscs," Proceedings, 24th International Geological Congress, Montreal, 1972.
[12] Oyawoye M.O., "The basement complex of Nigeria, In: Dessauvagie TFJ, Whiteman AJ (eds) African geology," Ibadan University Press, 1972.
[13] Odusanya B.O., Amadi U.N.P., "An empirical resistivity model for predicting shallow groundwater in the Basement Complex Water Resources," Journal of Nigeria Association of Hydrogeologists, **Vol. 2**, (1990), 77- 87.
[14] Satpathy B.N., Kanungo B.N., "Groundwater Exploration in Hard rock terrain, a case study," Geophysical Prospecting, **Vol. 24**(4), (1976), 725-736.
[15] Olorunfemi M.O., Olorunniwo M.A., "Parameters and aquifer characteristics of some parts of SW. Nigeria," Geologic Applica E. Hydrogeological, **XX** Part 1, (1985), 99-109.
[16] Dan-Hassan M.A., and Olorunfemi M.O., "Hydro-geophysical investigation of a basement terrain in the north central part of Kaduna State, Nigeria," Journal of Mining Geology, **Vol. 35**(2), (1999), 189-206.
[17] McNeill, J.D., "Electromagnetics," In Proceedings on the Application of Geophysics to Engineering and Environmental Problems, (1988), 251-348.
[18] Fraser, D.C., "Contouring of VLF-EM data," Geophysics, **Vol. 34**(6), (1969), 958-967.
[19] Karous M., Hjelt S.E., "Linear Filter of VLF Dip-Angle Measurements," Geophysical Prospecting, **Vol. 31**, (1983), 782-794.

[20] Philips, J. D., "Locating magnetic contacts: a comparison of Horizontal Gradient, Analytic signal, and Local wavenumber methods," Society of Exploration Geophysicists Expanded abstracts, 2000.

[21] Mogaji, K. A., Olayanju, G. M. and Oladapo, M. I., "Geophysical evaluation of rock type impact on aquifer characterization in the basement complex areas of Ondo State, Southwestern Nigeria: Geo-electric assessment and Geographic Information Systems (GIS) approach," International Journal of Water Resources and Environmental Engineering, **Vol. 3(**4), (2011), 77-86.

Appendix

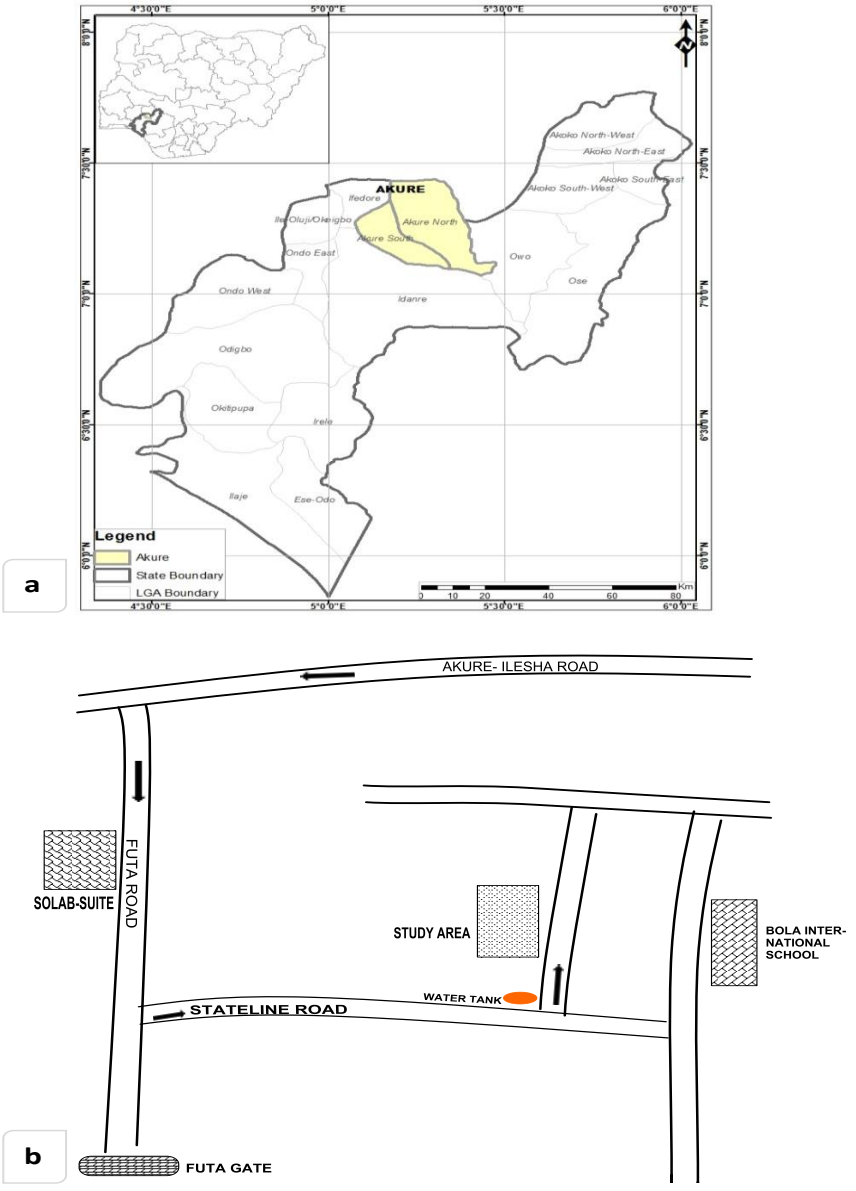

Figure A1: (a) The Map of Ondo state showing the study site modified after [21]. (b) Base map of the study site.

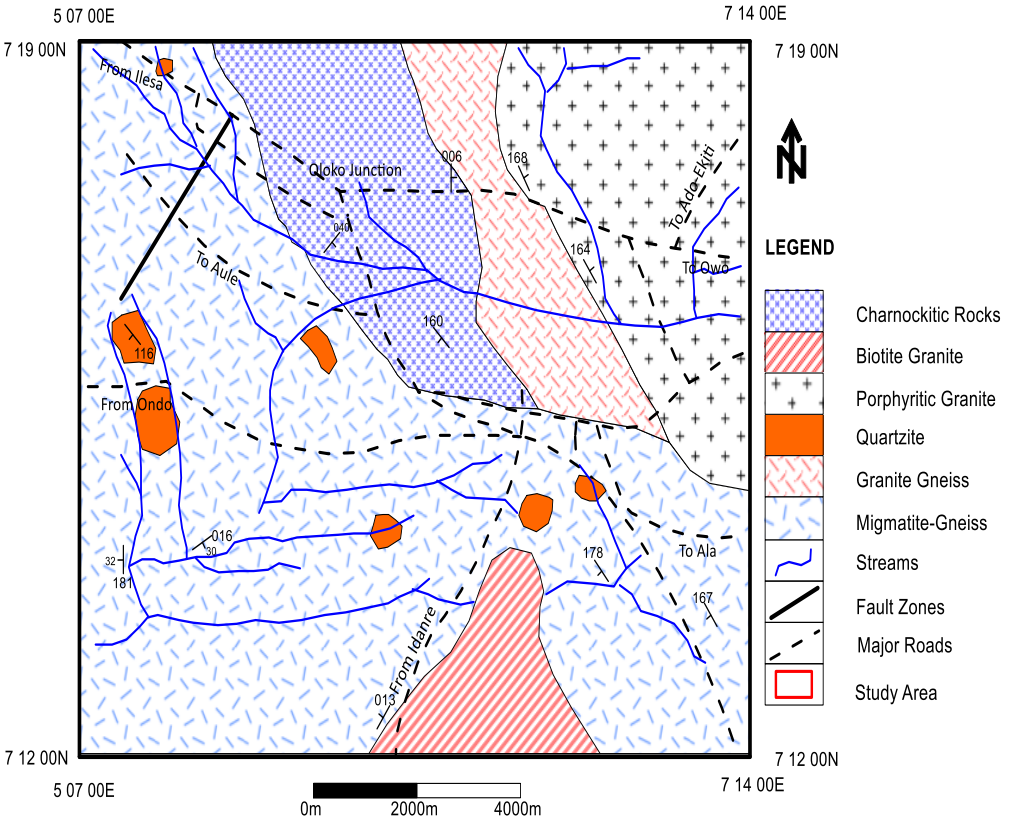

Figure A2: Simplified Geological map of Akure (After Owoyemi, 1996)

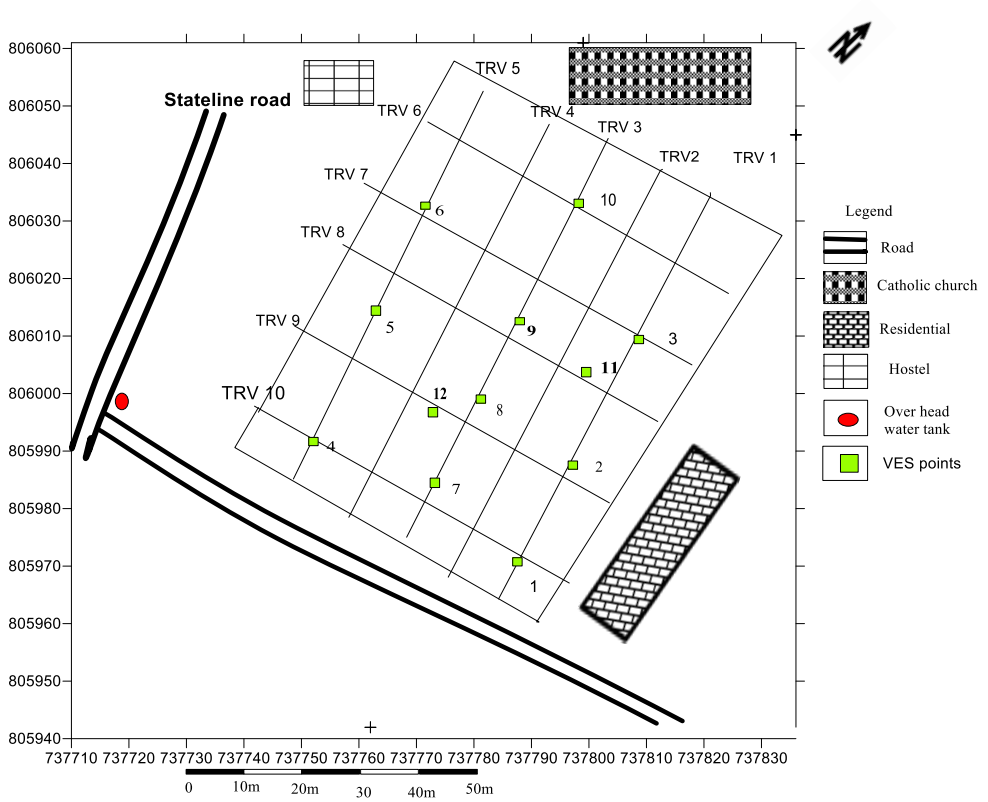

Figure A3: Survey design for the study site

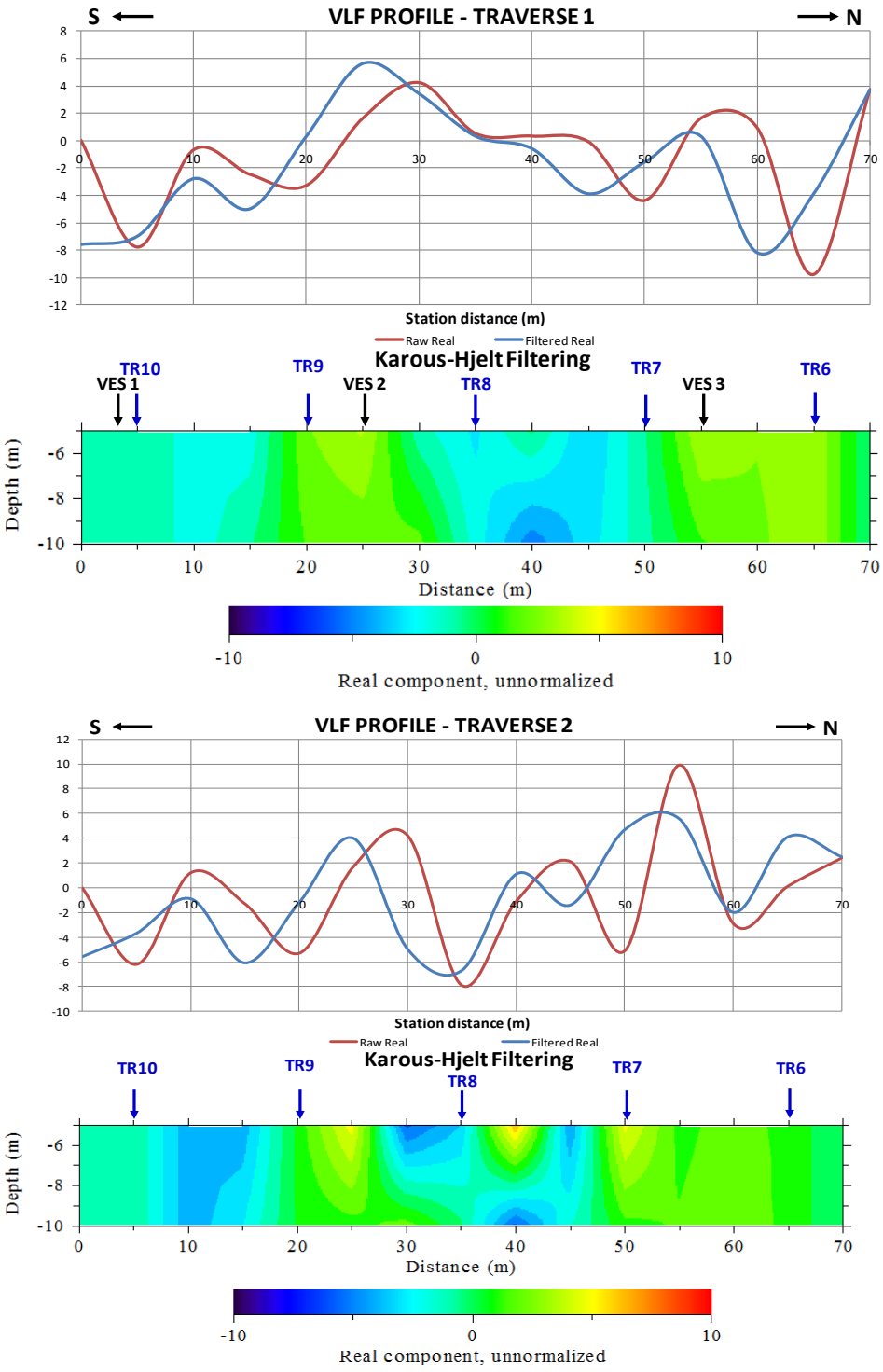

Figure A4a: VLF Profile and pseudo section along Traverse 9 and 10

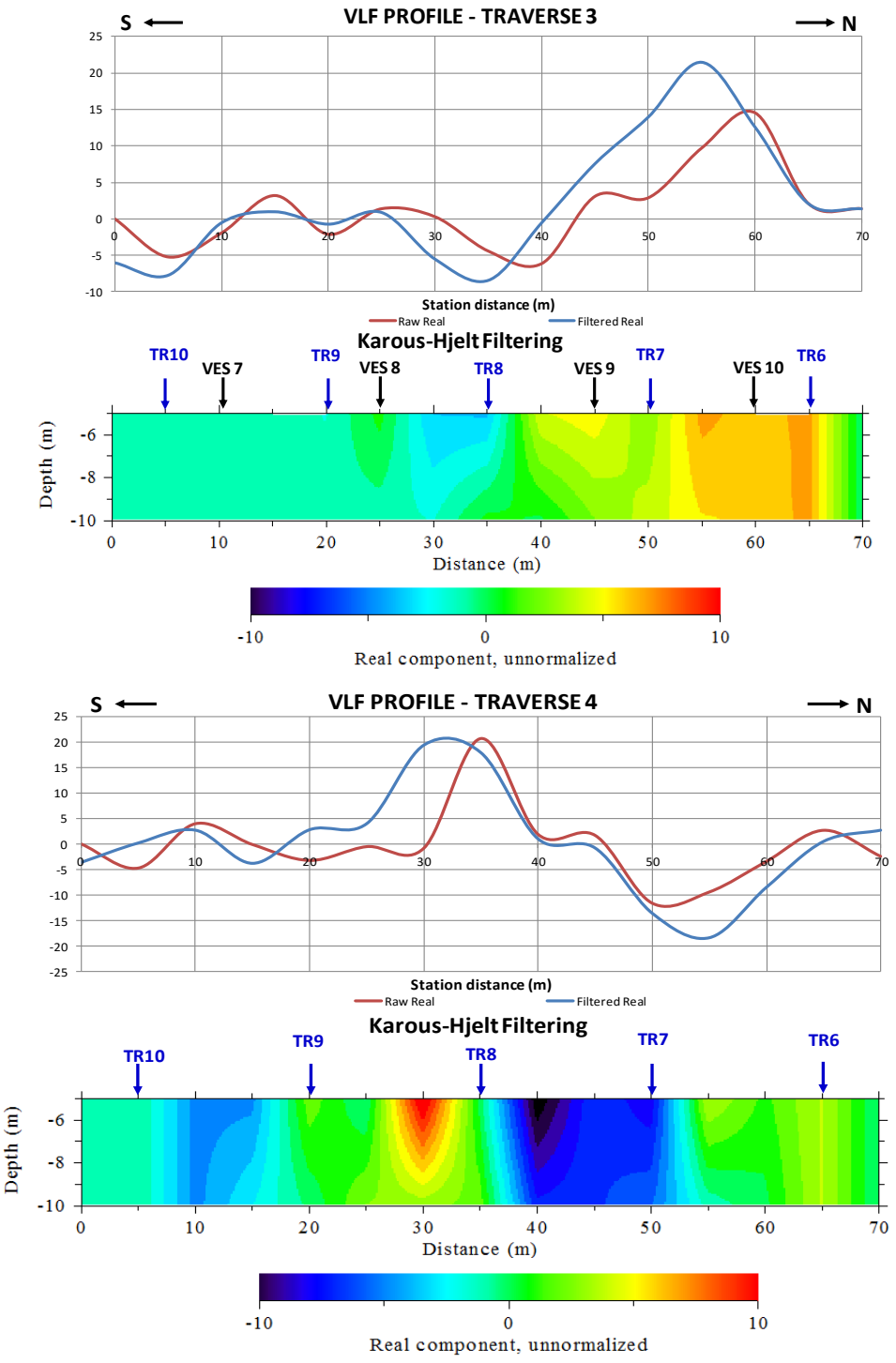

Figure A4b: VLF Profile and pseudo section along Traverse 9 and 10

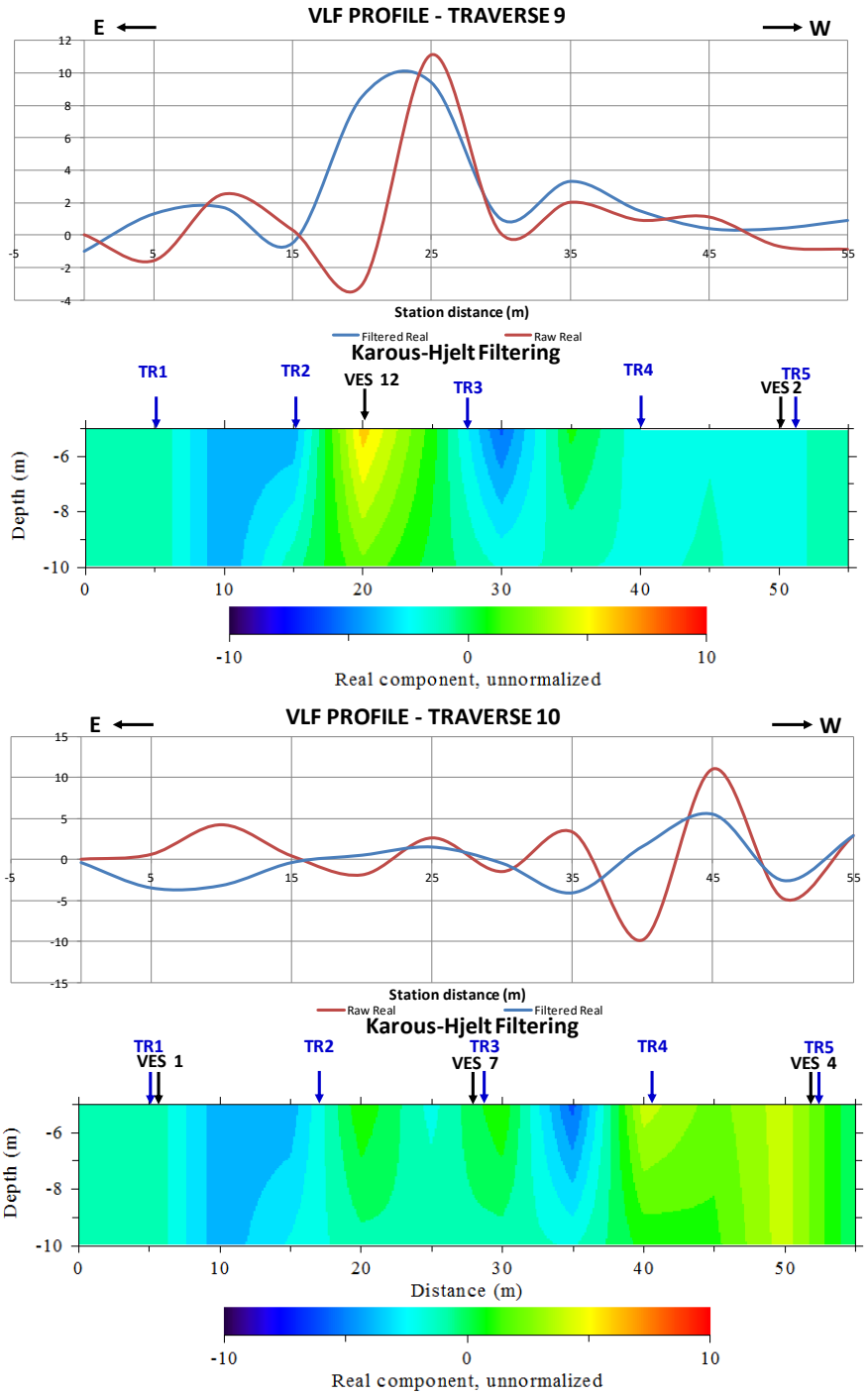

Figure A4c: VLF Profile and pseudo section along Traverse 9 and 10

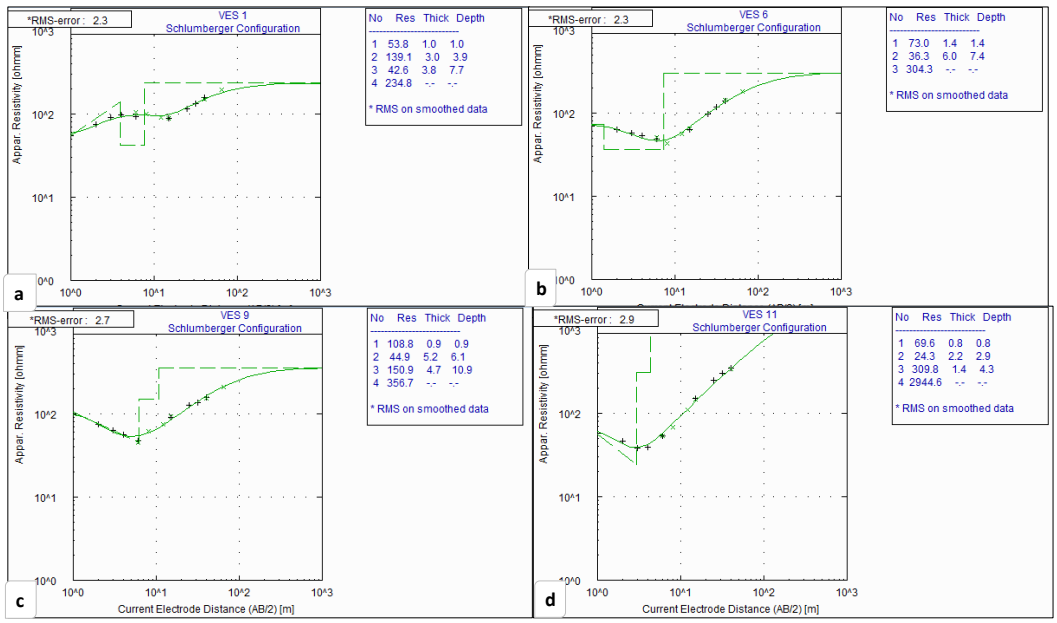

Figure A5: (a) VES 1 Typical 'KH' curve (b) VES 6 Typical 'H' curve (c) VES 11 Typical 'HA' curve and (d) VES 11 Typical 'HA' curve

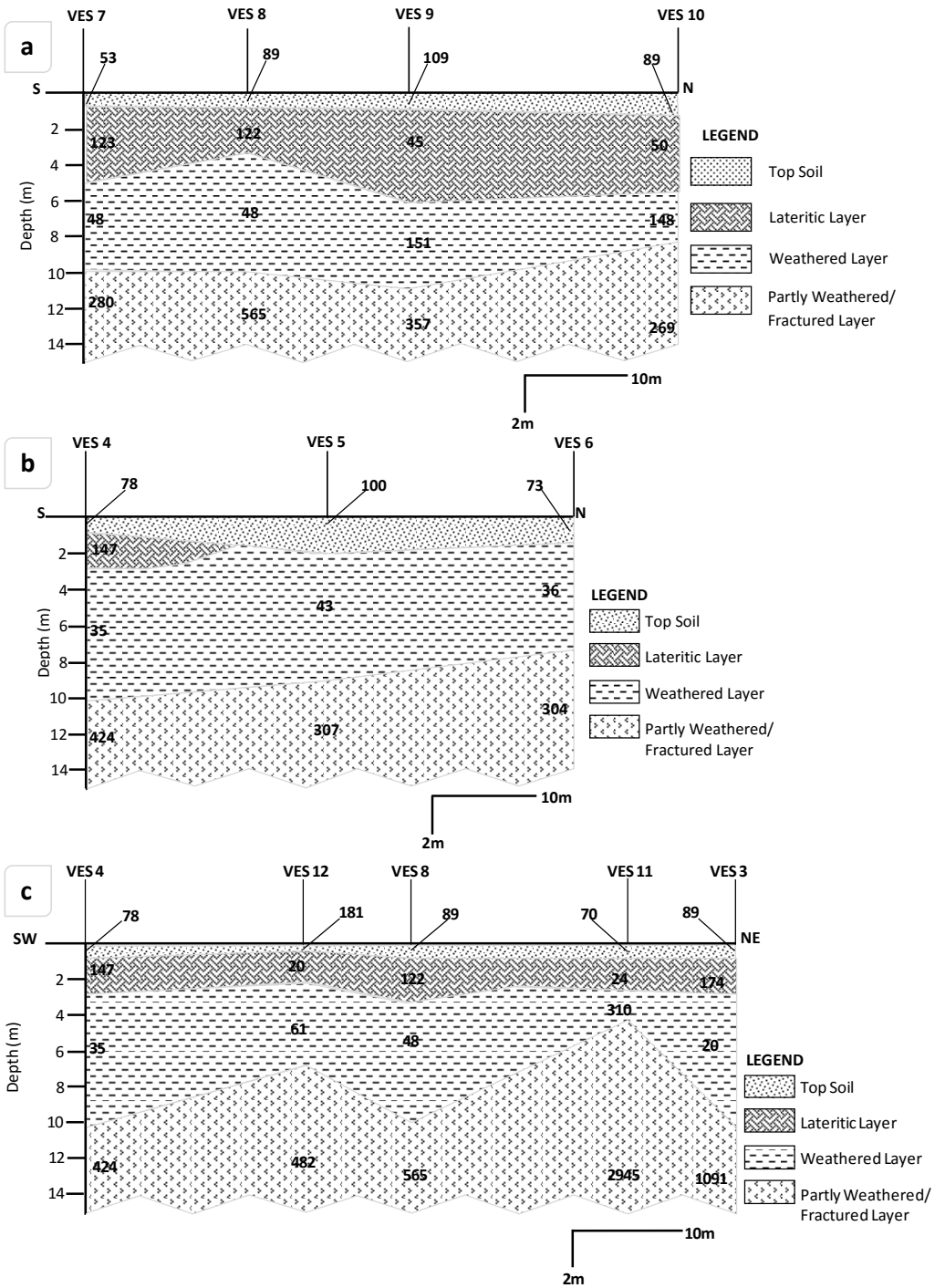

Figure A6: (a) Geo-electric section along traverse 3, (b) Geo-electric section along traverse 5 and (c) Geo-electric section along an arbitrary line intersecting VES 4, 12, 8, 11 and 3.

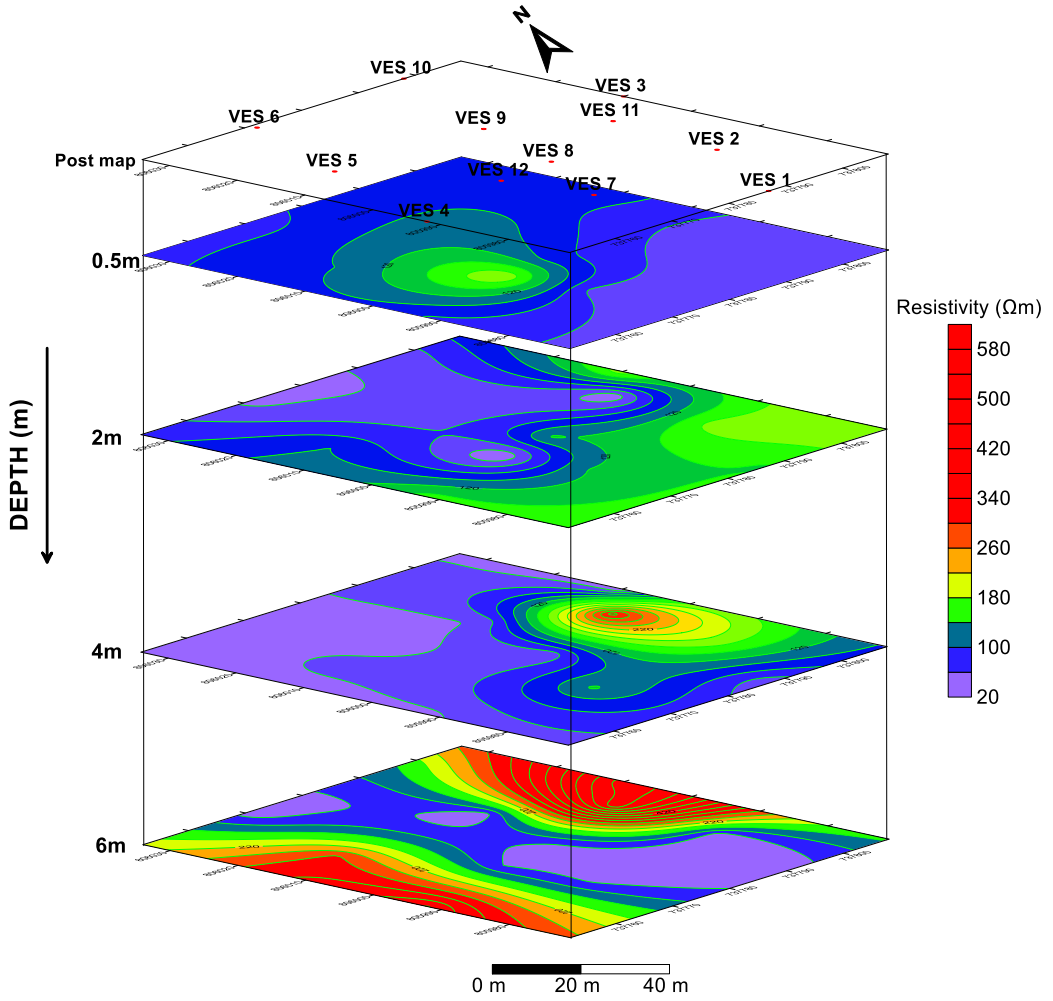

Figure A7: Post map over Iso-resistivity depth slice at 0.5, 2, 4 and 6 m. High resistivity value associated with the top of the basement rock is prominent at 4m.

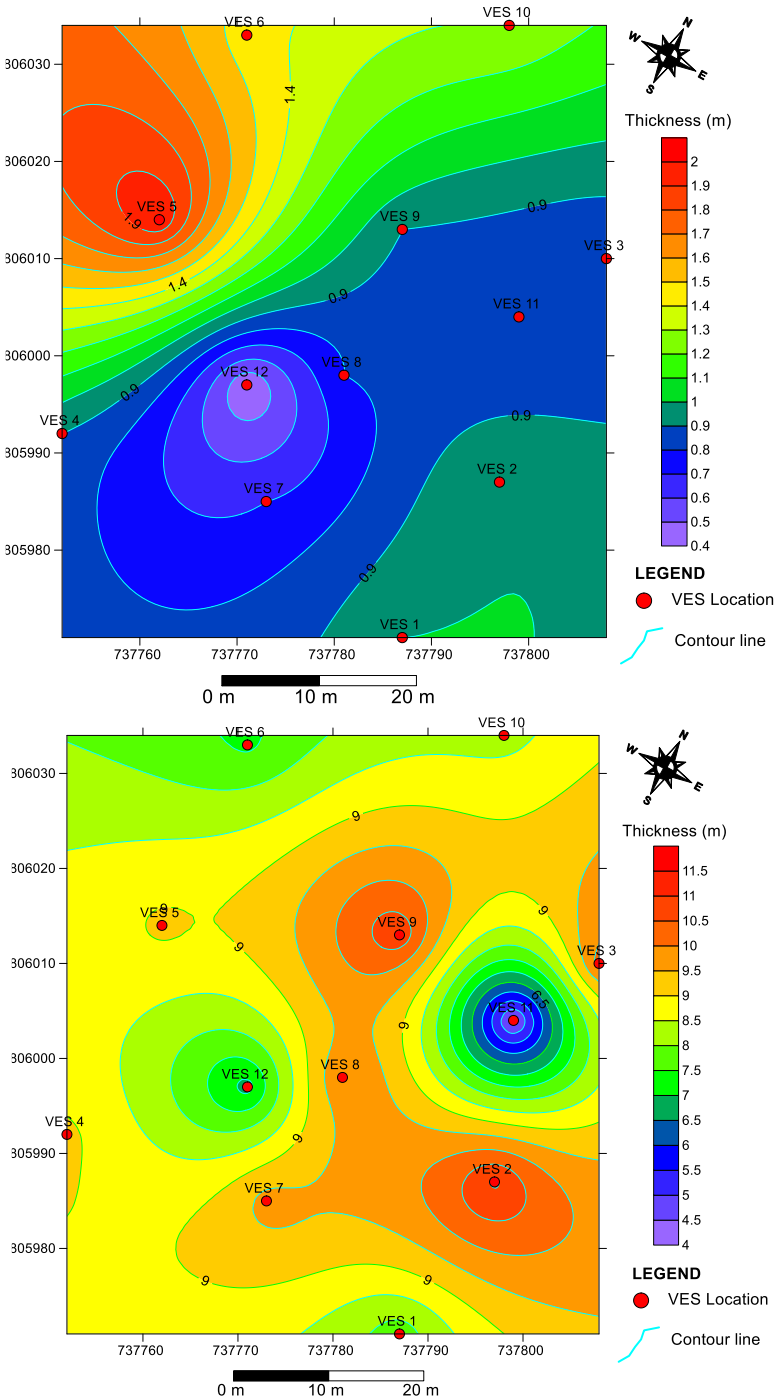

Figure A9: (a) Thickness map of top soil (b) overburden thickness map

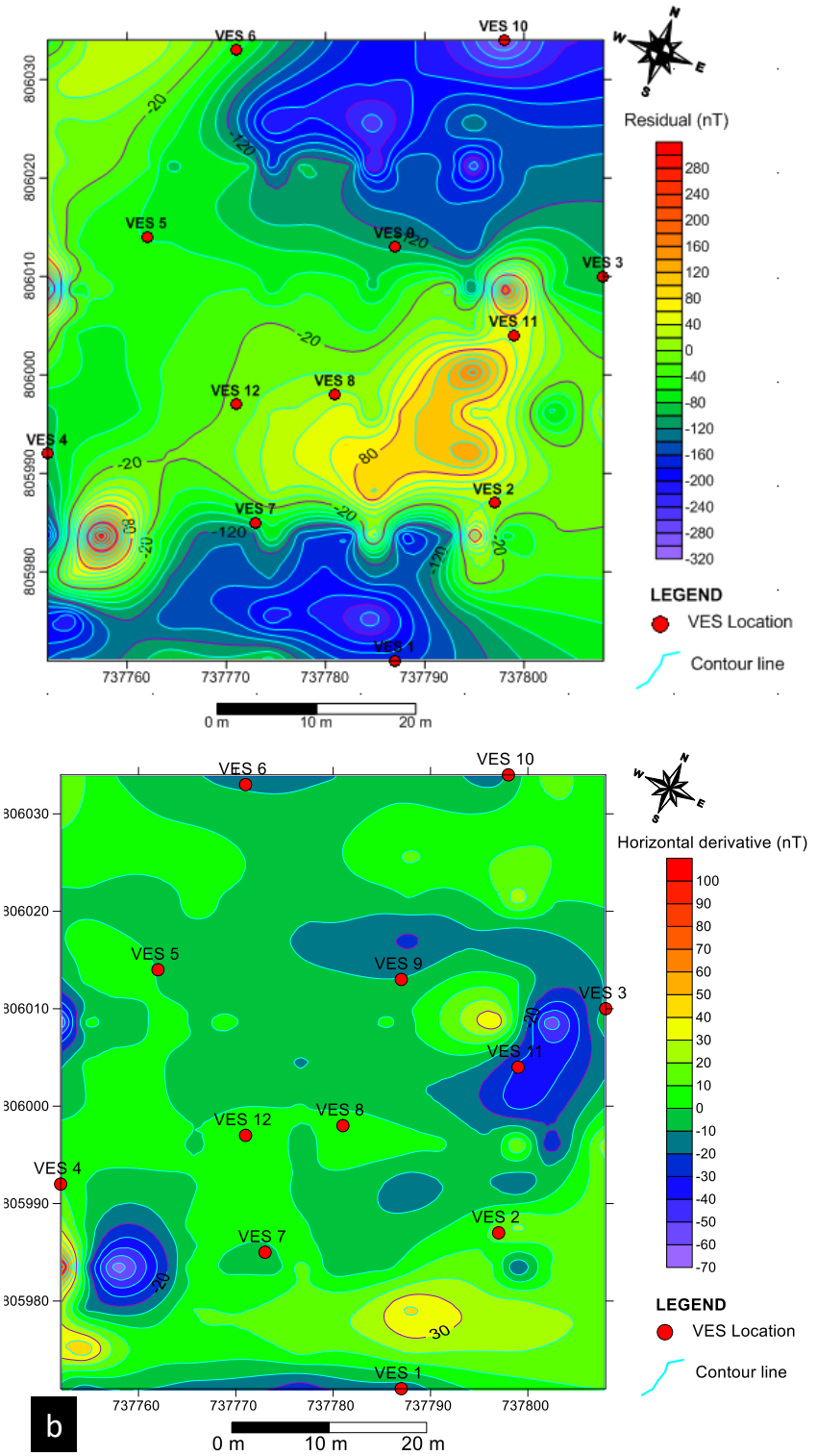

Figure A10: (a) Residual magnetic anomaly map (b) Horizontal derivative map of the magnetic anomaly.

Table A1: Summary of geo-electric parameters over the study area

VES Station	No. of layers	Resistivity (Ohm-m) $\rho_1/\rho_2/\ldots\rho_{n-1}$	Curve Type	Thickness(m) $h_1/ h_2/ h_3$	Depth(m) $d_1/d_2/\ldots d_{n-1}$
1	4	54/139/43/235	KH	1.0/2.9/3.8	1.0/3.9/7.7
2	4	44/170/39/220	KH	1.0/4.0/6.1	1.0/5.0/11.1
3	4	89/174/20/1091	KH	0.8/2.0/7.4	0.8/2.8/10.2
4	4	78/147/35/424	KH	0.9/2.8/5.5	0.9/3.6/9.1
5	3	100/43/307	H	2.0/7.1	2.0/9.1
6	3	73/36/304	H	1.4/6.0	1.4/7.4
7	4	53/123/48/280	KH	0.7/4.2/4.8	0.7/5.0/9.7
8	4	89/122/48/565	KH	0.8/2.5/6.7	0.8/3.3/10.0
9	4	109/45/151/357	HA	0.9/5.2/4.7	0.9/6.1/10.9
10	4	89/50/148/269	HA	1.3/4.5/2.5	1.3/5.6/8.3
11	4	70/24/310/2945	HA	0.8/2.2/1.4	0.8/2.9/4.3
12	4	181/20/61/482	HA	0.4/1.7/4.6	0.4/2.1/6.8